

Generative AI for Visualizing Highway Construction Hazards Through Synthetic Images and Temporal Sequences

Trevor Neece¹, Mason Smetana¹, and Lev Khazanovich¹

¹University of Pittsburgh, Pittsburgh, PA, USA

Abstract

Highway construction workers face a high risk of serious injury or death. Image-based training materials depicting hazardous scenarios are essential for engaging safety instruction but remain scarce due to ethical and logistical barriers. This study develops and evaluates a generative AI methodology for producing synthetic visualizations of highway construction hazards from OSHA Severe Injury Report narratives. Two modes were developed: a single-pass approach yielding one image per incident, and a temporal approach producing a four-stage sequence. A sample of 75 incident records yielded 750 images, evaluated using CLIP-based semantic retrieval and expert assessment across dimensions such as educational utility, fidelity, and alignment. Single-pass images achieved 81.1% educational acceptability with fidelity and alignment scores of 4.14/5 and 4.07/5, respectively, while temporal sequences achieved 60.9% acceptability with comparable alignment (3.94/5) but lower fidelity (3.51/5). CLIP-based retrieval revealed that both modes produce images with statistically significant retrieval capabilities. This is among the first studies to leverage modern autoregressive image generation models for visualizing construction hazards from reported severe injuries and to generate temporally sequenced hazard imagery, and a new multi-dimensional evaluation framework was developed to support future research in this domain. The work enables safety trainers to pair narrative storytelling with visual learning material without photographing real-world hazards, and the framework could be applied to datasets across diverse domains, enabling synthetic image generation tailored to new application areas.

Keywords: Generative AI, synthetic imagery, highway construction safety, workforce education, image evaluation.

1 Introduction

Workers in highway construction work zones are at very high risk of serious injury or death, with recent statistics showing that work zone fatalities increased by approximately 21.5% between 2015 and 2023 ([Work Zone Safety Information Clearinghouse, 2025](#)). Within a work zone, construction labor is conducted alongside live traffic, leading to interactions between workers and vehicles and thus increasing the risk of injury for both drivers ([Weng and Meng, 2011](#)) and workers ([Nnaji et al., 2020](#)). This labor is vital to the development of sustainable

built environments and to overall societal prosperity, as road and highway construction significantly impacts economic development (Gkritza et al., 2008). However, persistent safety risks indicate that the industry needs greater focus on safety-related research (Eseonu et al., 2018).

Workers tend to act based on their perception of risk, which is often misguided compared to the true risk (Asnar and Zannone, 2008). As such, calibrating a worker’s perceived risk with the objective risk of a highway construction task is a key driver of safety (Wilkins, 2011). Safety knowledge, therefore, is highly correlated with safety performance (Sawacha et al., 1999). Although health and safety training is common in construction, a major limitation is the overuse of ineffective presentation techniques such as text-based lectures. When high-engagement training, characterized by interactive and visually centered learning activities, is employed, skill training and safety knowledge acquisition are up to three times as effective compared to low-engagement methods (Burke et al., 2006). Given the elevated risks in work zones, safety instructors must be keenly aware of which methods keep learners engaged to ensure that vital safety knowledge is effectively communicated.

In a lecture or presentation setting, audience attention typically alternates between engaged and unengaged in cycles that often grow shorter as the session progresses (Bunce et al., 2010), and visually centered, high-engagement training has been shown to counteract these diminishing cycles (Albert et al., 2020). Techniques such as narrative-based training, where learners observe a construction hazard visually evolving over time and engage in discussions, can further enhance engagement and improve retention of safety knowledge (Eggerth et al., 2018). Safety-based storytelling, in which a safe construction scene transitions to a critical hazard, provides this narrative structure, giving learners the contextual buildup needed to recognize warning signs before a hazard peaks (Cullen, 2008). This format mirrors the real-world experience of a work zone, where hazards rarely materialize instantaneously but instead develop through a series of events that a trained worker should be able to identify and act upon. However, these techniques are often hindered by a fundamental data availability gap: there are very few high-quality image datasets of construction hazards (Guo et al., 2021). Capturing such imagery directly is constrained by site access limitations, the ethical problem that authentic photographs would document workers engaged in unsafe practices that should be interrupted rather than recorded, and companies’ reluctance to release any such imagery publicly. The drivers of this gap are discussed further in the literature review.

Although image data are scarce, large databases of text-based descriptions of construction hazards exist. For example, since 2015, OSHA has required U.S. employers to report all severe occupational injuries, including location, incident description, and injury details (Gomes et al., 2023). With advanced image-generation capabilities enabled by methods such as Stable Diffusion and generative artificial intelligence (AI), such text-based descriptions can be transformed into images (Acharjee et al., 2025). By leveraging generative models, the industry can bypass the ethical and logistical hurdles of capturing real-world images of hazards. Consequently, these synthetic visuals can be integrated into the high-engagement, narrative-based training modules previously discussed, providing workers with vivid, contextually relevant training material. Synthetic images would address many data availability gaps and provide a scalable framework for calibrating worker risk perception, potentially reducing fatalities.

Despite the promise of generative AI, stochastic models exhibit substantial variance in their outputs. In some applications, this variability can be modulated via a “temperature” parameter; however, for tasks that require creativity, such as image generation, such control is not always feasible or desirable (Li et al., 2025). A single-attempt image generation will often produce a pedagogically incorrect image on the first iteration, as text-to-image models frequently struggle with fine-grained semantic alignment and complex spatial reasoning in a single pass (Khan

et al., 2025). Instead, achieving reliable output typically requires an iterative process in which initial generations are evaluated and refined (Jeon et al., 2025). The following section situates this work within the broader literature on safety training, synthetic image generation in construction, and the evaluation of AI-generated imagery, and identifies the gaps this study aims to address.

1.1 Literature Review

Building on the engagement and data-scarcity issues outlined above, prior work has further established that high-engagement methods are especially effective for high-exposure occupations such as highway construction (Burke et al., 2011), and that interactive multimedia outperforms lecture-based training while being cost-effective to redeploy across sessions (Cherrett et al., 2009; Albert and Routh, 2021). The corresponding shortage of hazard imagery has multiple drivers: expert annotation is expensive (Ricketts et al., 2023), site cameras are positioned for coverage rather than detail (Tian et al., 2024), and companies withhold imagery for liability reasons (Tanga et al., 2022). Methods for generating project-specific hazard visualizations are therefore needed to fill this gap.

Accordingly, the generation of synthetic images for diverse datasets containing hazardous scenarios is a recently emerging research topic. Lee et al. (Lee et al., 2022) leveraged game-engine renderings of construction machines imposed onto synthetic backgrounds to create a new dataset of heavy machine operations. Xiong et al. (Xiong and Tang, 2021) used game-engine-generated dust effects and layered them only on construction images for dataset augmentation, achieving an F1 score of 0.93 when a YOLO-v3 model trained exclusively on 3,860 synthetic images was evaluated against 1,015 real-world construction photographs. Wei et al. (Wei and Akinci, 2021) developed a BIM-to-game-engine framework for generating synthetic images of construction projects using digital ground truth. Kim et al. (Kim and Yi, 2024) used text-to-image generative models to create a dataset of 3,585 hazardous images spanning 27 hazard categories, then trained a deep neural network to process images for hazard recognition, achieving a mean average precision of approximately 64% in object detection and 60% in segmentation. Neece et al. (Neece and Fascetti, 2026) used game-engine-based images of construction hazards from construction health and safety training modules as benchmarking data for AI-based image hazard identification, reporting that 95% confidence intervals for model recognition scores substantially overlapped between real and synthetic image classes across all three multimodal AI models evaluated, indicating statistically similar performance. Collectively, these studies demonstrate that synthetically generated construction imagery, produced via game engines, BIM pipelines, or generative AI, yields performance competitive with real-world data.

Generative models (e.g., diffusion-based or autoregressive models) have demonstrated capabilities in text-to-image synthesis and offer a pathway to producing synthetic imagery that bypasses traditional data collection barriers. Hong et al. (Hong et al., 2024) similarly used a stable diffusion model (Diffusion SDXL 1.0 model with the Huggingface diffusers library) to create images representing construction tasks, and found that 82.01% of synthetic images were suitable representations of the desired task. Additionally, a CNN model trained on synthetic images with and without context-based labels saw classification accuracy of 89.09% and 86.51%, respectively. Acharjee et al. (Acharjee et al., 2025) generated images of general workplace-specific accident scenarios using accident narratives from OSHA’s Severe Injury Reports (SIRs) with Stable Diffusion 3.5 Large. The workflow involved large language models (LLMs) for generating descriptions of accident scenarios and a pretrained diffusion model for

creating new image/label pairs. The methodology was evaluated by manual inspection, which found that 86% of images accurately represented the scenario described in the corresponding prompt. This work acknowledges a limitation of standard diffusion: although the generated images capture the intended hazards, they often appear overly artistic rather than photorealistic.

Developments in text-to-image generation by frontier AI developers accelerated significantly in late 2025, with new autoregressive models enabling the generation of images with superior visual quality (Zuo et al., 2025). Along with improvements in fidelity, new models can produce image-to-image translations without degrading the original input (Xiao et al., 2025). The core challenge in image-to-image generation has historically been that diffusion models re-synthesize the entire image during denoising, such that regions the user did not want to change are subject to stochastic variation. Recent frontier multimodal LLMs, such as Google’s Gemini 3 Pro (Google DeepMind, 2025c), have demonstrated region-specific editing capabilities, enabling localized semantic modifications to target image regions while preserving the structural and appearance fidelity of non-target content. As such, consistent image-to-image generation enables the generation of sequential images that depict how hazards evolve, without degradation of vital image components, such as construction tasks and highway infrastructure.

While generative AI shows significant promise in creating image-based visualizations that do not yet exist, vision-language models (VLMs) exhibit known limitations in spatial reasoning (Kamath et al., 2023) and domain-specific accuracy in construction (Adil et al., 2025), which must be addressed for reliable application in safety-critical training contexts. Kamath et al. evaluated 18 vision-language models on spatial reasoning tasks (i.e., reliably distinguish between “right” vs “left”) and found that all performed poorly (Kamath et al., 2023). Neece et al. (Neece and Fascetti, 2026) demonstrated that VLMs have a baseline capability for hazard recognition, but perform worse in identifying electrocution and struck-by hazards.

To evaluate synthetic imagery, Otani et al. found that most studies use automated evaluation metrics to validate generated images or rely on human evaluation, which lacks repeatability (Otani et al., 2023). Additionally, their work defined best practices for evaluating AI-generated images, specifically a 1-5 Likert-scale human grade for fidelity and alignment. Cook et al. proposed a checklist-based evaluation methodology that increased agreement between LLM-based and human-based evaluations of generated content (Cook et al., 2024). Lu et al. generated synthetic construction images of construction machinery and validated the new dataset using a quantitative computer-vision-based recall assessment and a qualitative expert-based Turing Test (Lu et al., 2025). Within the highway construction domain, expert-based evaluation criteria are underdeveloped for safety-related applications (Neece et al., 2026).

The studies reviewed above establish that synthetic imagery can serve as a substitute for photographs for construction safety. However, training applications require both technical validity and educational utility. As established in the introduction, high-engagement visual training significantly outperforms lecture-based instruction in both knowledge acquisition and retention (Burke et al., 2006), and narrative-based techniques, in which learners observe a hazard visually unfolding over time, further enhance engagement and the practical application of safety knowledge (Cullen, 2008; Eggerth et al., 2018). A static image of a hazard does not maximally fulfill this narrative function. Ideally, multiple images would depict how hazards evolve over time, providing narrative cues for workers to learn from. Despite growing interest in AI-generated imagery for construction, no prior work has considered the generation of temporally sequenced hazard imagery depicting the progressive escalation from safe conditions to critical safety violations. Additionally, highly realistic safety-based images have not yet been evaluated using an expert-based framework in the highway construction domain.

1.2 Research Aims and Objectives

There is a clear gap in the availability of image-based safety training materials depicting hazardous highway construction scenarios. While OSHA’s databases provide a rich corpus of historical incident narratives, no established methodology systematically transforms these records into visual training assets. Concurrently, recent advances in frontier image generation models have demonstrated region-specific editing capabilities and high-fidelity image-to-image translation that were not previously achievable, creating a new technical opportunity for synthetic safety visualization. This study, therefore, addresses the following research question: How can generative AI be leveraged to produce realistic, structurally coherent, and semantically valid synthetic imagery of construction safety hazards that evolve over time, and what methodologies should guide the evaluation of such imagery?

The key contributions of this study, illustrated in Figure 1, are as follows:

1. A framework for single-pass generation of highway construction hazard imagery using structured prompt engineering, in which a layered prompting strategy decomposes complex hazard scenes into infrastructure, activity, and hazard elements to produce photorealistic imagery from a single text-to-image generation pass.
2. A framework for generating temporal image sequences that depict hazard progression, from safe configurations through early-warning states to critical violations, using iterative image-to-image conditioning to maintain visual continuity across sequential frames.
3. A framework for both automated and manual evaluation of synthetic construction safety imagery, addressing dimensions such as fidelity, alignment, educational utility, and retrieval.

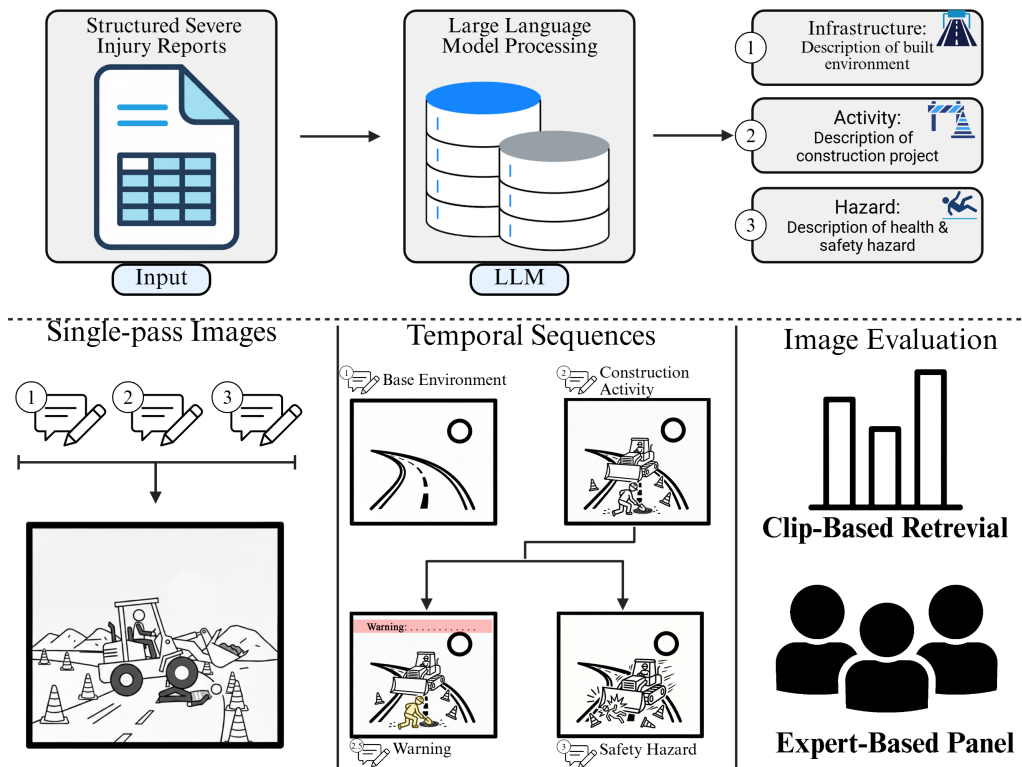


Figure 1: Graphical overview of the proposed contributions of this study.

2 Methodology

The proposed methodology is illustrated in Figure 2. OSHA SIRs serve as the primary input, processed by an LLM f_θ to produce structured scene descriptions, which are then fed into two distinct image generation pipelines. In Mode I, a single-layered extract drives a one-pass generation through the image generator f_G , producing I_{SP} . In Mode II, four sequential descriptions (R_{T1} , R_{T2} , R_{T3} , and R_{T4}) drive an iterative image-to-image conditioning pipeline, yielding the temporal sequence $\{I_{T1}, I_{T2}, I_{T3}, I_{T4}\}$. The resulting images are then evaluated using two complementary strategies: CLIP-based retrieval and an expert-based panel, as described in Section 2.5.

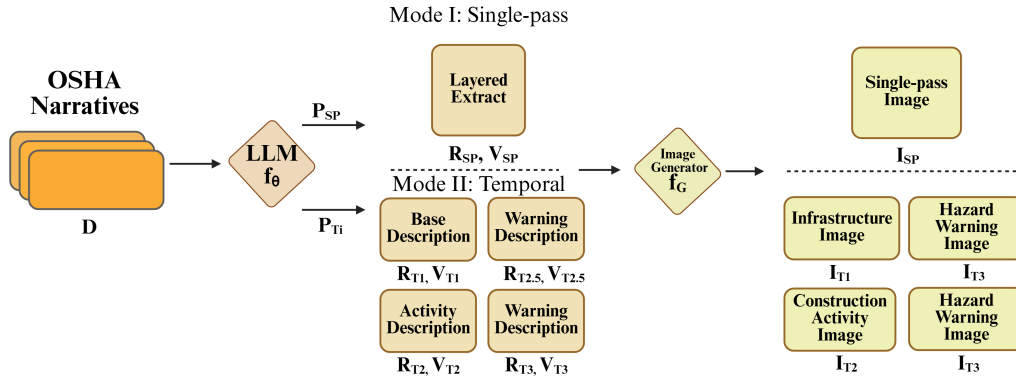


Figure 2: Overview of the proposed methodology, illustrating the flow from OSHA SIR narratives through LLM-based scene description generation to two image generation pipelines (Mode I: Single-pass and Mode II: Temporal).

2.1 Severe Injury Reports for Highway Construction

The OSHA SIRs were used as the ground-truth data source for generating images. This database was selected for its completeness and text-rich abstracts that describe the reported severe injury. The OSHA SIR database, spanning 2015–2021, contains more than 70,000 records across all North American Industry Classification System (NAICS) industry codes. For this study, only NAICS Code 237310 was used, which corresponds to Highway, Street, and Bridge Construction. After filtering, 1198 structured incidents were collected for potential inclusion.

Each incident record D drawn from the narratives dataset is treated as a structured document containing 26 fields:

$$D = \{\text{site_address}, \text{abstract_text}, \text{event_keyword}, \text{src_of_injury}, \text{event_type}, \dots\}$$

While fields such as “abstract_text”, “event_keyword”, and “src_of_injury” carry the majority of the scene-relevant information, administrative fields such as “activity_nr”, “reporting_id”, and “summary_nr” are included on the basis that their presence does not degrade generation quality, and that manual selection of fields would introduce unnecessary subjective choice. Smetana et al. (Smetana et al., 2024, 2026) previously analyzed this dataset using LLMs across the same NAICS 237310 subset, identifying the free-text investigator narrative (field “abstract_text”) as the primary source of analytical value and validating its semantic richness for downstream LLM tasks.

To evaluate semantic alignment between generated images and their source descriptions, a random sample of 75 SIR records was drawn from this dataset. Based on the “event_keyword”

field, the sample was dominated by Struck-By incidents ($n = 37$), followed by Fall from Elevation ($n = 10$), Caught in/Between ($n = 9$), Other ($n = 7$), and Struck Against ($n = 6$), with five smaller categories accounting for the remaining six records.

For each of the 75 selected records, two independent image generation iterations were executed under both modes described in Sections 2.3 and 2.4. That is, for each incident record D , this resulted in 10 images: two single-pass hazard representations and two temporal sequences of four images each. The two iterations per methodology used identical prompts and visual constraints, differing only in the stochastic variation inherent in the image generator, allowing within-method consistency to be measured and quantifying how much semantic variability arises from generation stochasticity versus from differences in source records. The image generation was performed in February 2026.

2.2 Generative AI Models

This study employed two generative AI models. The text generator, denoted by f_θ , was Google’s Gemini 2.5 Flash (Google DeepMind, 2025a), selected for its low latency and cost efficiency for structured outputs. The image generator, denoted as f_G , was Google’s Gemini 3 Pro (Google DeepMind, 2025b), selected for its superior visual fidelity and region-specific editing capabilities required by the temporal pipeline. The methodology can, in principle, replace either f_θ or f_G with any model capable of instruction-following text generation and image-to-image generation, respectively. Models were accessed via the Google Generative AI API, with a fixed temperature of 0.0 for f_θ to minimize stochastic variation across incident records, ensuring that differences in generated output are attributable to differences in the source data D rather than sampling noise. For f_G , the default temperature setting was employed to enable stochastic variety in image generation, as recommended in the Gemini 3 Pro documentation (Google DeepMind, 2025c).

2.3 Mode I: Single-pass Image Generation

This initial methodology generates an image from the raw incident record D in one pass, rather than employing image-to-image scene composition. The complete record D is passed to f_θ with a structured prompt P_{SP} that instructs the model to define three narrative layers:

1. The Infrastructure: The base roadway or work zone layout (e.g., pavement, lane markings, traffic control), with no mention of machines or workers.
2. The Activity: The construction equipment and workers performing their routine task within that space.
3. The Hazard: the peak of the event, focusing on the physical interaction between the worker and the hazard.

The model is instructed to generate 1-2 sentences per narrative layer and produce a cohesive response using the three descriptions, producing the output R_{SP} . Additionally, the model is instructed not to dramatize or invent information outside of that provided in the incident report. As such, the output of the first structured prompt can be represented as:

$$R_{SP} = f_\theta(P_{SP}(D))$$

This description is then embedded in a visual constraints prompt V_{SP} . This prompt is always the same for each unique R_{SP} . The visual constraints prompt instructs the image generator f_G to generate the single-pass image I_{SP} according to a few key rules:

1. The image should be a photorealistic educational visualization of the construction scenario, taken at eye level, as if the inspector were standing a few feet away.
2. The image must be “locked” at this perspective, and not panned or zoomed.
3. The focal point (workers, vehicles, the incident, etc.) must be the sharpest and most distinct part of the image.
4. The activity and hazard elements must be integrated seamlessly into the infrastructure, without introducing unnecessary environmental clutter.
5. There must be no overlaid text, labels, or captions. Text must appear only on physical objects within the scene, such as on signs.

As such, the methodology for single-pass image generation can be represented as:

$$I_{SP} = f_G(V_{SP} + R_{SP})$$

Figure 3 (A) presents four representative images generated via the single-pass pipeline, each produced from a distinct SIR incident record. The generated scenes depict a range of highway construction hazard types. In each case, the layered prompting strategy integrated infrastructure, activity, and hazard elements into a single coherent scene, with workers and equipment spatially positioned to reflect the described incident interaction. The first image depicts a construction vehicle crushed by a mismanaged crane load; the second and fourth images depict a worker run over by a backing vehicle; the third image depicts a roller that lost control while coasting down a hill and struck a tree.

2.4 Mode II: Temporal Sequence Generation

The temporal methodology decomposes each incident record D into a set of four temporally ordered descriptions $\{R_{T1}, R_{T2}, R_{T3}, R_{T4}\}$, each generated by the language model f_θ conditioned on D and prior outputs. The four stages are:

- R_{T1} : the static base environment, including road surface, lane markings, terrain, and traffic control layout, with all workers and equipment suppressed.
- R_{T2} : the populated work zone, introducing workers and equipment into the base environment in positions consistent with the impending hazard.
- R_{T3} : an annotation identifying the at-risk worker and a concise warning phrase describing the upcoming hazard, branched from R_{T2} .
- R_{T4} : the hazard event, depicting the worker/hazard interaction described in the source SIR record.

These descriptions then drive a sequential image-generation pipeline. The first state T_1 , is generated from D alone:

$$R_{T1} = f_\theta(P_{T1}(D))$$

States 2 and 4 are generated sequentially using the previous text description and D :

$$R_{T2} = f_\theta(P_{T2}(D, R_{T1}))$$

$$R_{T4} = f_{\theta}(P_{T4}(D, R_{T2}))$$

R_{T3} is also conditioned on R_{T2} but instead produces an annotation specification: the identity and position of the at-risk worker to be highlighted, and a concise warning phrase of 5–7 words describing the upcoming hazard. As such:

$$R_{T3} = f_{\theta}(P_{T3}(D, R_{T2}))$$

Both R_{T3} and R_{T4} branch from R_{T2} independently:

$$R_{T3} \leftarrow R_{T2} \rightarrow R_{T4}$$

Each text description is added to a visual constraints prompt $\{V_{T1}, V_{T2}, V_{T3}, V_{T4}\}$ and passed to the image generator f_G . V_{T1} instructs f_G to generate a photorealistic eye-level photograph of the base environment only, with no workers or equipment, a clean minimalist background, and no overlaid text or UI elements. V_{T2} instructs f_G to modify I_{T1} via image-to-image generation, integrating workers and equipment seamlessly into the existing scene while locking the camera angle, perspective, and focal length to maintain visual consistency with I_{T1} . V_{T2} also embeds R_{T4} as a spatial positioning constraint, requiring that workers and equipment be placed such that the hazard described in R_{T4} can realistically occur in the subsequent frame, without depicting the hazard itself. V_{T3} instructs f_G to modify I_{T2} by adding two annotation layers only: a red outline or glow around the at-risk worker identified in R_{T3} , and a high-contrast safety warning banner displaying the warning phrase in the upper or lower third of the image. V_{T4} instructs f_G to modify I_{T2} to depict the hazard event, allowing the camera angle to be adjusted to ensure the worker-hazard interaction is clearly visible, while preserving the background scene. The full temporal image generation pipeline can therefore be represented as:

$$\begin{aligned} I_{T1} &= f_G(V_{T1} + R_{T1}) \\ I_{T2} &= f_G(I_{T1}, V_{T2} + R_{T2} + R_{T4}) \\ I_{T3} &= f_G(I_{T2}, V_{T3} + R_{T3}) \\ I_{T4} &= f_G(I_{T2}, V_{T4} + R_{T4}) \end{aligned}$$

Figure 3 (B) presents four representative temporal image sequences, each consisting of four frames generated from a single SIR incident record (corresponding to the same four incidents shown in panel A). Across all four sequences, the infrastructure and scene geometry established in the first frame are consistently preserved in subsequent rows, demonstrating the visual continuity maintained by the iterative image-to-image conditioning pipeline.



(A)



(B)

Figure 3: Examples of highway construction images generated from the SIR database. (A) single-pass images and (B) temporal sequences. Stages of temporal sequence indicated by numbers (1, 2, 3, and 4).

2.5 Evaluation

Two complementary evaluation strategies were employed to assess the quality of the synthetic highway construction safety images. The first was an automated evaluation using CLIP (Contrastive Language–Image Pre-training) (Radford et al., 2021), which measures the semantic alignment between generated images and their source text descriptions in a shared embedding space. The second was an expert-based evaluation, in which domain experts rated generated images across multiple quality dimensions. Together, these evaluations provide both quantitative retrieval metrics and qualitative assessments of image quality.

2.5.1 CLIP-Based Semantic Alignment Evaluation

To assess how well the generated images capture the semantic content of their source incident descriptions, a retrieval evaluation was performed using OpenAI’s CLIP ViT-L/14 model (Radford et al., 2021). CLIP was not fine-tuned on construction safety imagery or SIR incident narratives specifically. As such, any retrieval performance above chance reflects semantic alignment learned from the model’s pretraining rather than domain-specific knowledge. The CLIP model employed herein limits all text-based inputs to 77 tokens (approximately 50-60 words). Accordingly, using the entire SIR record as the text-embedding component was not feasible. The text label for this analysis concatenates the “event_description” field, which provides a concise event summary (e.g., “Employee’s leg fractured when struck by falling beam”), with

the abstract field, truncated to fit the 77-token window. Prior to concatenation, the abstract field was preprocessed using a series of regular expression substitutions to remove common patterns such as date/time preambles, employee identifiers, and company names, thereby using the remaining token budget on hazard-relevant content. Additionally, for temporal sequence-based images, only the stage 4 image (I_{T4}) was embedded for evaluation. The assumption was that any semantic errors present in I_{T1} or I_{T2} propagate through the image-to-image editing process, making evaluation of I_{T4} alone an adequate proxy for assessing the entire sequence.

Cosine similarity in CLIP’s shared 768-dimensional embedding space was computed between L2-normalized image and text embeddings:

$$\text{sim}(I, T) = \mathbf{e}_I \cdot \mathbf{e}_T = \sum_{d=1}^{768} e_{I,d} e_{T,d}$$

Liang et al. (Liang et al., 2022) demonstrated that CLIP’s image and text encoders embed their outputs into separate regions of the shared space, producing a positive baseline similarity even between unrelated images and descriptions. As a result, a cosine similarity between an image and a text must be compared against the baseline similarity of unrelated pairs to determine whether the match is meaningful.

Cosine similarity-based evaluation was measured in the text-to-image (T2I) retrieval direction, in which each of the 75 preprocessed text descriptions served as a query and was directly compared against a gallery of 300 synthetic images. This gallery comprised, for each incident, two single-pass hazard images and two temporal stage 4 hazard images, yielding four correct-target images per query. As such, for each D , 300 images I were ranked by cosine similarity, and retrieval performance was evaluated with respect to these four correct targets.

An empirical null distribution was constructed from all mismatched (non-corresponding) image-text pairs. That is, the 75 text queries correspond to 296 non-corresponding images, yielding $75 \times 296 = 22,200$ mismatched pairs. Additionally, a distribution was constructed from all matched pairs, since each of the 75 text queries corresponds to 4 images, yielding $75 \times 4 = 300$. Cosine similarity between these embeddings in the shared CLIP space was calculated and characterized by its mean, standard deviation, and percentiles. The cosine similarity of matched pairs was directly compared with a Mann-Whitney U significance test, where $p < 0.05$ indicated similarities that are unlikely to arise from unrelated image-text pairings in this domain. This test assumes independence of observations and equal distributional shape under the null hypothesis. Additionally, this was a one-tailed test, as the null hypothesis states that matched similarities are no greater than mismatched similarities. Rejection of the null hypothesis would indicate that the generated images encode the semantic content from the source material, beyond what would be expected from visually similar but contextually different construction safety scenes. To quantify the practical magnitude of the separation between matched and mismatched distributions, Cohen’s d is reported as an effect size measure:

$$d = \frac{\mu_{\text{match}} - \mu_{\text{mismatch}}}{\sqrt{\frac{\sigma_{\text{match}}^2 + \sigma_{\text{mismatch}}^2}{2}}}$$

where μ and σ denote the mean and standard deviation of each group, respectively. The widely used convention is that $d = 0.2$ is considered a small effect, $d = 0.5$ a medium effect, and $d = 0.8$ a large effect (Cohen, 2013). Additionally, retrieval performance was quantified using Mean Reciprocal Rank (MRR) and Recall at k ($R@k$). MRR measures the average inverse rank of the first correct result, and $R@k$ measures the proportion of queries for which at least one correct item appears in the top k results.

2.5.2 Expert-Based Image Evaluation

A panel of six domain experts with experience in highway construction safety independently evaluated the AI-generated image sets, with three professionals in construction safety and three students in civil engineering. Each image set was assessed by at least two reviewers. Due to varying availability among expert evaluators, the number of evaluations completed per rater was not uniform; however, the minimum dual-rater coverage across all items ensured that no assessment relied on a single evaluator’s judgment.

Reviewers were presented with a pair of images (or a pair of temporal sequences), both generated using the same image-generation methodology (i.e., single-pass or temporal) and both generated from the same SIR record (D). Generated images were evaluated using a structured assessment comprising three distinct sections. The first section was a checklist-based hallucination search. A hallucination, in this context, refers to a feature in the image that does not accurately match the input incident description or the construction work zones in general. Following a curated list of typical hallucinations relevant to highway construction safety hazard images, reviewers identified whether each hallucination type was present in the image. Providing a binary checklist-based criterion for image evaluation is a more structured and effective approach for identifying errors compared to ad hoc identification (Chaudhary et al., 2025; Cook et al., 2024). Images were assessed across four dimensions (single-pass) or six dimensions (temporal):

1. Processing Artifacts: watermarks, overlaid text, unwanted photographer elements.
2. Hazard Accuracy: depicted hazard matches the SIR record (Steps 2-4 for sequences).
3. Scene Realism: logically arranged elements consistent with a real highway work zone job site.
4. Visual Coherence: physically plausible renderings.
5. Temporal Consistency¹: stable people/equipment across Steps 2-4.
6. Hazard Alert Accuracy¹: Step 3 overlay correctly identifies and describes the at-risk worker.

For all questions, a yes/no response was required, with “yes” indicating that the specific type of hallucination was not in the image/sequence. When a “no” response was given, the rater was instructed to provide an explanation of the hallucination. Figure 4 (A-E) shows several examples of the hallucinations described in the expert survey.

¹Temporal sequence evaluation only.



Figure 4: Examples of hallucinations by category: (A) processing artifact: head and shoulder of worker taking photo is visible, (B) processing artifact: Google Street View watermarks are visible, (C) scene realism: work zone setup is illogical, and the welding tool is plugged into the excavator head, (D) visual coherence: worker and machine wheel are abnormally large, (E) temporal consistency: bundle of wood duplicates between images.

Once the reviews were completed, for each binary checklist item (coded as 1 if the image was free of the specified hallucination or 0 if the hallucination was present), the pass-rate was computed as the percent of all individual ratings coded as 1, across both iterations within each method (single-pass and temporal). To quantify inter-rater reliability, Cohen's κ was computed for each dimension. Since most image sets were evaluated by two reviewers while a subset received three or four evaluations due to varying reviewer availability, κ was computed via Light's method (Light, 1971), which takes the mean of all pairwise Cohen's κ values within each image set and thereby incorporates all available ratings rather than discarding those beyond the first. Agreement strength was interpreted using the Landis and Koch thresholds: below 0.20 as slight, 0.21–0.40 as fair, 0.41–0.60 as moderate, 0.61–0.80 as substantial, and above 0.80 as almost perfect (Landis and Koch, 1977).

The second phase of the evaluation was a direct comparison of educational utility between the two images. Reviewers assessed the overall suitability of each image as an educational visualization of the described construction hazard, using a three-tier scale: “No Issues – Fully Acceptable”, “Minor Issues – Still Acceptable”, and “Major Issues – Not Acceptable”. Reviewers were also asked to provide written justification for their educational utility ratings. Educational ratings were defined as the image’s ability to serve as a visual representation of the hazard in classroom discussions. Hallucinations, when present in a synthetic image, do not necessarily affect the educational value of the image. Accordingly, reviewers were instructed that hallucinations did not automatically invalidate the educational value if the hazard interaction remained clear. To examine which hallucination types most strongly influenced educational utility judgments, checklist failure rates were cross-tabulated against the three educational utility categories.

The third and final phase, following recommendations from Otani et al.’s best practices for human evaluation of text-to-image generation (Otani et al., 2023), had reviewers provide scalar ratings of the hazard image (Step 4 for sequences; the single image for single-pass) for fidelity and alignment. Fidelity was rated on a 1-5 Likert scale, anchored by “Looks like an AI-generated photo” and “Looks like a real photo”. Alignment (that is, semantic agreement with the SIR report) was rated on a 1-5 Likert scale anchored by “Does not match at all” and “Matches exactly”. For both scales, means and standard deviations were computed across all ratings pooled within each methodology. To characterize inter-rater variability on the Likert scales, the mean absolute difference between paired reviews ($|\Delta|$) was reported, representing the average magnitude of disagreement in scale points between two reviewers evaluating the same image.

3 Results

After applying the image generation methodology to both Mode I (single-pass) and Mode II (temporal) to the 75 randomly selected OSHA narratives, 750 images were created in total. This comprises 150 single-pass images (each of the 75 narratives producing two images) and 600 temporal images (each of the 75 narratives was used twice to create two sequences of four images). All images were of resolution 1408×768 , consuming an average disk space of 933 KB, and total disk space of 684 MB.

3.1 CLIP-based Semantic Alignment

The empirical null distribution, constructed from 22,200 mismatched image-text pairs, and visualized in Figure 5 (A), was characterized by a mean cosine similarity of $\mu = 0.178$ and standard deviation $\sigma = 0.044$. The positive null mean is consistent with the modality gap phenomenon described by Liang et al. (Liang et al., 2022), in which CLIP’s image and text encoders embed their outputs onto geometrically separated cones in the shared space, producing a positive baseline similarity even between unrelated pairs. Matched image/text pairs had a mean cosine similarity of $\mu = 0.249$, and a standard deviation of $\sigma = 0.040$. The mean separation is 1.48σ above the null mean. Additionally, the effect size was confirmed by the Mann-Whitney U test, yielding a highly significant p-value (1.22×10^{-106}). As such, the null hypothesis was rejected. The cosine similarity scores between correctly matched image-text pairs were greater than those between mismatched pairs. This result indicates that the image generation model encoded the source incident description into the synthetic image. This conclusion is supported

by a Cohen’s d of 1.545, which is substantially greater than the baseline for a “large” effect size. Separated by single-pass and temporal (see Figure 5 (B) and (C)), the effect size remains large for both single-pass ($d = 1.755$) and temporal ($d = 1.366$), with the null hypothesis rejected in both cases ($p < 10^{-47}$). Full distributional statistics for the overall and per-methodology comparisons are reported in the supplementary files.

The substantial overlap between matched and mismatched distributions in Figure 5 reflects the homogeneity of the construction-safety domain: because all images and queries originate from the same domain, even non-corresponding pairs share substantial visual and textual content. The meaningful result, therefore, is the consistent rightward shift in matched pairs and the statistically significant effect size.

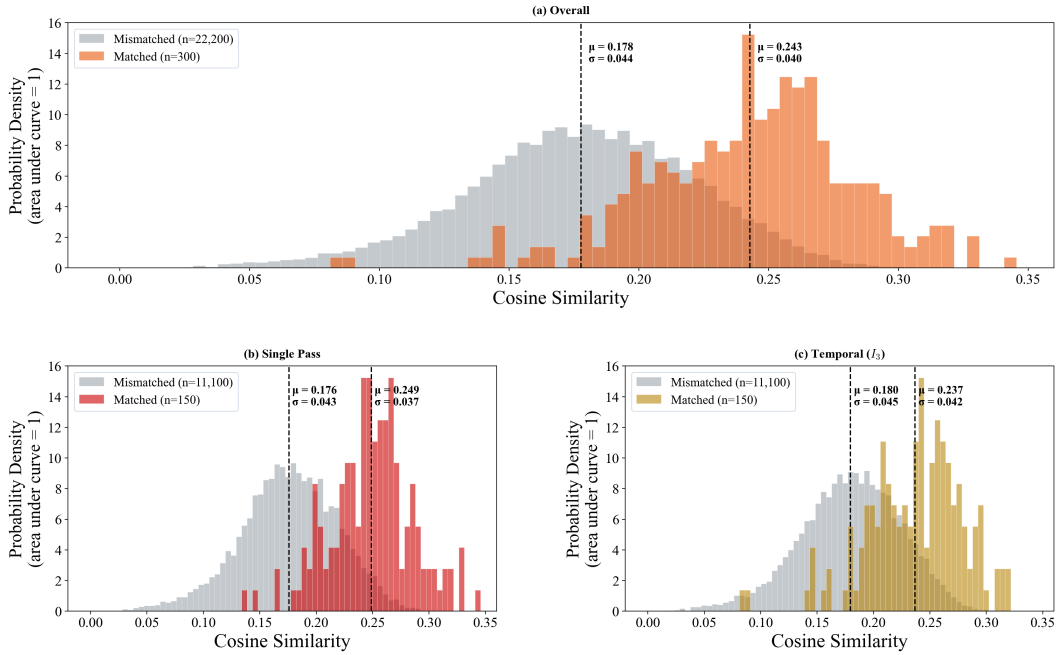


Figure 5: Distribution of cosine similarity scores between CLIP-encoded text descriptions and generated images, (A) overall, (B) single-pass images, and (C) temporal images, segmented by corresponding and non-corresponding pairs.

Table 1 summarizes the T2I retrieval performance. The pipeline achieved an MRR of 0.247 for text/image matches overall, an R@1 of 11.7%, and an R@10 of 54.3%, meaning that over half of all queries had at least one of their correct images ranked within the top 10 out of 300 candidates. The single-pass variant outperformed the temporal variant across all metrics, with an MRR of 0.293 versus 0.201 and R@1 of 16.0% versus 7.3%. This pattern held across all recall depths, with the single-pass variant achieving 64.0% at R@10, compared to 44.7% for the temporal variant.

Table 1: Text-to-image retrieval performance for CLIP-encoded text descriptions against the gallery of 300 generated images. Distributional separation statistics for matched vs. mismatched pairs are reported in the supplementary files.

Group	<i>n</i>	MRR	R@1	R@5	R@10
Overall	300	0.247	11.7%	37.3%	54.3%
Single-pass	150	0.293	16.0%	42.7%	64.0%
Temporal	150	0.201	7.3%	32.0%	44.7%

3.2 Expert-based Evaluation

Table 2 (A) summarizes the checklist-based hallucination assessment, with inter-rater agreement statistics reported in the supplementary files. Processing artifacts were the least prevalent hallucination type, with pass rates of 94.9% for single-pass images and 84.1% for temporal sequences, and inter-rater agreement in the moderate-to-substantial range. Hazard accuracy, which assessed whether the depicted hazard interaction reflected the incident described in the source SIR record, was the weakest dimension for both modes, with pass rates of 62.5% and 60.2% for single-pass and temporal images, respectively. Inter-rater agreement on hazard accuracy was fair, with Cohen’s κ values of 0.286 and 0.348, suggesting that reviewers applied moderately different thresholds when judging semantic alignment. Scene realism exhibited the lowest inter-rater agreement of any dimension ($\kappa < 0.20$ for both modes), despite a pass rate of 79.2% for single-pass images. For temporal sequences, scene realism dropped to 54.9%, as expected, since generating more images increases the likelihood that at least one has an unrealistic feature. Temporal consistency, assessed only for temporal sequences, had a pass rate of 59.9% with moderate agreement ($\kappa = 0.430$), the highest among the subjective dimensions. Hazard alert accuracy, which evaluated whether the Step 3 warning overlay correctly identified the at-risk worker and described the impending hazard, achieved the highest temporal-specific pass rate at 86.1% and fair agreement between reviewers.

Table 2: Expert evaluation summary by methodology. (A) Per-dimension pass rates and fail-in-major rates from the checklist assessment. (B) Overall educational acceptability and Likert-scale fidelity and alignment ratings. Inter-rater agreement (κ) and the full Fully/Minor/Major breakdown are reported in the supplementary files.

(A)

Dimension	Pass Rate (%)		Fail-in-Major (%)	
	Single-Pass	Temporal	Single-Pass	Temporal
Processing Artifacts	94.9	84.1	11.1	20.5
Hazard Accuracy	62.5	60.2	93.7	75.8
Scene Realism	79.2	54.9	36.5	51.5
Visual Coherence	87.7	82.0	17.5	28.8
Temporal Consistency	—	59.9	—	61.4
Hazard Alert Accuracy	—	86.1	—	26.5

(B)

Measure	Single-Pass	Temporal
Overall Educational Acceptability	81.1%	60.9%
Fidelity (Likert, $\mu \pm \sigma$)	4.14 \pm 1.05	3.51 \pm 1.35
Alignment (Likert, $\mu \pm \sigma$)	4.07 \pm 1.13	3.94 \pm 1.24

Table 2 (B) reports overall educational acceptability by methodology. Single-pass images were rated Fully Acceptable in 47.0% of evaluations and Acceptable with Minor Issues in 34.1%, yielding an overall acceptance rate of 81.1%. Temporal sequences scored 27.2% Fully Acceptable and 33.7% Minor Issues, for an overall acceptance rate of 60.9% (full distribution in the supplementary files). The Fail-in-Major column of Table 2 (A) reports, for each dimension, the proportion of image sets rated “Major Issues” in which that dimension was flagged, revealing which hallucination types most strongly correlate with educational rejection. Hazard accuracy emerged as the dominant predictor of educational rejection: for single-pass images rated “Major Issues,” 93.7% had a hazard accuracy failure, compared to only 1.3% of images rated “Fully Acceptable.” For temporal sequences, the same pattern held at 75.8% versus 4.3%. Scene realism and visual coherence failures, by contrast, plateaued between the “Minor Issues” and “Major Issues” categories for single-pass images, suggesting that reviewers sometimes tolerate these issues when the hazard itself is correctly depicted. For temporal sequences, temporal consistency joined hazard accuracy as a strong driver of rejection, with a failure rate of 61.4% among “Major Issues” ratings compared to 9.8% among “Fully Acceptable” ratings.

Likert-scale fidelity and alignment ratings are reported in Table 2 (B). Single-pass images received a mean fidelity rating of 4.14 with a standard deviation of 1.05. For alignment, single-pass images scored a mean of 4.07 with a standard deviation of 1.13. The mean absolute difference values were 0.84 and 0.89 for fidelity and alignment, respectively, indicating that paired reviewers typically disagreed by approximately one scale point, consistent with the inherent subjectivity of holistic image quality assessment. For temporal image sequences, the mean responses for fidelity and alignment were 3.51 and 3.94, with standard deviations of 1.35 and 1.24, respectively. Similar to single-pass images, the mean absolute difference was approximately one scale point. The key difference in results between modes is that temporal images exhibited a 4.8x greater reduction in mean fidelity score (-0.63) than in alignment score (-0.13). Generating synthetic images as a sequence, accordingly, increases the odds that the

output scores lower on photorealistic quality, but does not proportionally reduce the semantic alignment between the generated image and its source incident description. This suggests that the image-to-image conditioning pipeline introduces visual artifacts and degradation that reviewers perceive as less realistic, while largely preserving the scene’s hazard-relevant content.

A stochastic recovery analysis was conducted based on the comparative evaluations (see the full report in the supplementary files). For each paired assessment, the two iterations were categorized independently by each evaluator. As such, a pair of images (or sequences) can be categorized as “Both acceptable”, “Mixed”, or “Both rejected”. For single-pass images, 70.1% of paired assessments had both iterations rated as acceptable, 22.2% were mixed, and only 7.8% had both iterations rejected. For temporal sequences, 44.0% had both iterations acceptable, 33.3% were mixed, and 22.6% had both rejected. The recovery rate, defined as the proportion of mixed pairs among all pairs in which at least one iteration was rejected, was 74.0% for single-pass and 59.6% for temporal.

4 Discussion

The evaluation results indicated that generative AI has strong capabilities to create useful safety hazard visualizations that do not currently exist, and can therefore improve current health and safety training curricula. The first principal finding of this work was that CLIP-based analysis confirms that the synthetic images are encoded semantically with the safety content beyond chance (Cohen’s $d = 1.545$). Despite the visual homogeneity of the dataset, matched image/text pairings were statistically distinguishable from mismatched pairs across all conditions ($p < 10^{-47}$; see Table 1), validating the methodology as viable for generating semantically retrievable images. Retrieval performance, however, was moderate: the overall MRR of 0.247 indicates that the first correct result appeared around the 4th position on average, and R@1 reached only 11.7%. At broader recall depths, performance improved substantially, with R@10 exceeding 50% overall. It should be noted that CLIP was not tuned on construction safety imagery, and its 77-token input limit required truncation of the incident narratives, both of which likely suppressed retrieval performance.

A second principal finding was that the domain experts rated a majority of the generated images as educationally acceptable for use in safety training. Single-pass images achieved an overall acceptability rate of 81.1%, compared to temporal images with a lower but still majority acceptability rate of 60.9%. Cross-tabulating checklist failures against educational utility ratings revealed that hazard accuracy was the primary determinant of whether an image was judged educationally viable. Hazard accuracy failure rates increased greatly from the “Fully Acceptable” to the “Major Issues” categories for both modes, while scene realism and visual coherence failures did not exhibit the same change. This suggests that reviewers tolerate imperfections in the surrounding environment when the hazard interaction itself is correctly depicted. Additionally, stochastic recovery analysis revealed that when at least one iteration was rejected, the alternative iteration generated from the same record and identical prompt was acceptable in 74.0% of single-pass cases and 59.6% of temporal cases. This indicates that generation quality is not solely determined by the source incident record but also by stochastic randomness in image generation. As such, future research on developing an automated system to identify and regenerate unacceptable images would be a valuable contribution to this domain.

Thirdly, single-pass images outperform temporal sequences across all quantitative metrics. Temporal sequences offer a unique capability in construction education: narrative progression and storytelling, which have the potential to increase engagement and knowledge retention (Eg-

gerth et al., 2018). However, because each frame in the temporal pipeline is conditioned on the output of the previous step, errors introduced in earlier stages propagate throughout and compound, increasing the likelihood that at least one frame in the sequence contains a hallucination. For instance, Street View interface artifacts that occasionally appeared in Stage 1 outputs persisted through every subsequent frame. Temporal sequences were also subject to two additional checklist dimensions (temporal consistency and hazard alert accuracy), and thus to additional scrutiny. Notably, this compounding degradation manifests primarily in fidelity rather than alignment.

Beyond the image generation methodology itself, this study contributes an expert-based evaluation framework for synthetic construction safety imagery. The checklist-based hallucination assessment, informed by Cook et al.'s finding that structured criteria improve evaluation consistency (Cook et al., 2024), decomposed image quality into inspectable dimensions rather than holistic judgments. Inter-rater agreement, as measured by Light's kappa, varied substantially across dimensions (see supplementary files). Dimensions involving binary judgments, such as processing artifacts and temporal consistency, achieved moderate to substantial agreement, whereas more subjective dimensions, such as scene realism and visual coherence, exhibited only slight agreement. This pattern suggests that the latter dimensions, as currently defined, may be too broad to elicit consistent judgment between experts.

For single-pass images, the 81.1% acceptability rate, together with the 74.0% recovery rate, suggests that generating two iterations per incident record will, in most cases, yield at least one educational, viable image without prompt refinement. For temporal sequences, the narrative progression from a safe base environment through an activity state to a hazard event aligns directly with the discussion-based training format identified by Burke et al. (Burke et al., 2011) and Cullen (Cullen, 2008) as most effective for high-hazard occupations.

Several relevant limitations must be acknowledged. First, the Mann-Whitney U test assumes independence of observations, which is partially violated by the repeated appearance of each image across mismatched pairs; however, the extreme significance ($p < 10^{-47}$) provides a substantial margin. Second, the results are specific to Google's Gemini 3 Pro image generation model as accessed in February 2026; given the rapid pace of development in frontier image generation, future models may address many of the hallucination types identified herein. Only one multimodal embedding model was evaluated for retrieval metrics (OpenAI's CLIP ViT-L/14), and performance may vary with newer models of different architectures. Additionally, the rater panel of six evaluators (three construction professionals and three civil engineering students) exhibited substantial imbalance in rating volume: two reviewers completed approximately 83% of all evaluations, while the remaining four contributed 17%. This imbalance was a consequence of varying availability rather than a design choice. Annotating safety-related construction images is a skilled task that often requires manual labor; as such, automated metrics should be further explored, given the scarcity of human annotators. Lastly, the evaluation assessed educational suitability as judged by domain experts and retrieval performance through CLIP-based analysis, but did not measure downstream training effectiveness.

Several directions for future research are enabled by this study. First, iterative prompt refinement using a secondary vision-language model to evaluate generated images and adjust the input prompt accordingly, as proposed by Jeon et al. (Jeon et al., 2025), could improve educational acceptability. Second, a training effectiveness study comparing text-based instruction, image-based instruction, and synthetic-image-based instruction would help determine whether the educational acceptability, as evaluated by domain experts, translates into knowledge retention. Third, the evaluation framework developed herein could be refined by decomposing scene realism and visual coherence into more specific sub-criteria to improve inter-rater agreement,

and by expanding the rater panel to include a broader range of construction safety professionals. Lastly, expanding the methodology beyond NAICS code 237310 (Highway, Street, and Bridge Construction) or to other datasets in different scientific fields would test the generalizability of the proposed frameworks.

5 Conclusion

This study addressed the research question of how generative AI can be used to create realistic and semantically valid imagery of highway construction safety hazards that evolve over time, as well as what modes should guide the evaluation of these images. Three contributions were presented.

First, a structured prompt engineering framework for the single-pass generation of synthetic images depicting highway construction hazards was defined. Single-pass images achieved an overall educational acceptability rate of 81.1% from the domain expert panel, as well as mean fidelity and alignment scores of 4.14/5 and 4.07/5, respectively. Additionally, a CLIP-based retrieval analysis showed that single-pass synthetic images exhibit statistically significant semantic alignment relative to the null mean.

Second, a temporal image generation pipeline to produce four images in a sequence to depict (1) a safe base environment, (2) active construction, (3) early-warning for a hazard event, and (4) a hazardous construction event leading to severe injury was developed. Temporal sequences achieved an educational acceptability rate of 60.9%, with mean fidelity and alignment scores of 3.51/5 and 3.94/5, respectively. Similar to single-pass images, CLIP-based analysis revealed a statistically significant semantic alignment relative to the null mean. The results indicate that narrative-based synthetic visualization is feasible, but compounding errors across sequential images leads to more hallucinations than single-pass generation.

Third, a multi-dimensional evaluation framework that combines CLIP-based semantic retrieval with an expert-based educational utility grade was developed. Cross-tabulation revealed that hazard accuracy was the dominant predictor of educational rejection across both modes. This finding provides clear guidance for future prompt engineering efforts: accurate depiction of the worker/hazard interaction matters more to educational value than photorealistic rendering of the surrounding scene.

These results demonstrate that generative AI can transform text-based narratives into visual training assets and address the data scarcity of images depicting dangerous construction activities. The methodologies enable safety instructors to produce project-specific, hazard-focused visualizations without photographing active hazards in real construction sites. As frontier image generation models continue to improve, the image generation framework and the evaluation guidelines established in this study provide a foundation for tracking how these improvements translate into gains in educational utility for highway construction safety training.

Funding

The findings reported here are based on work performed with the support of the Impactful Resilient Infrastructure Science & Engineering (IRISE) consortium in the Department of Civil and Environmental Engineering, Swanson School of Engineering at the University of Pittsburgh. We are indebted for the advice and assistance provided by the following representatives of IRISE member organizations that comprised the technical panel who guided work on the project: Pennsylvania Turnpike Commission, Pennsylvania Department of Transporta-

tion, Contractors Association of Western Pennsylvania, Michael Baker International, Allegheny County, Golden Triangle Construction, and the Federal Highway Administration.

References

- Sanjay Acharjee, Abir Khan Ratul, Diego Patiño, and Md Nazmus Sakib. Data-driven safety: Leveraging historical accident data and generative ai to generate workplace hazard scenarios. In *Computing in Civil Engineering 2025: Resilient, Robotic, and Educational Systems*, pages 847–856. 2025.
- Muhammad Adil, Gaang Lee, Vicente A Gonzalez, and Qipei Mei. Using vision language models for safety hazard identification in construction. *arXiv preprint arXiv:2504.09083*, 2025.
- Alex Albert, Idris Jeelani, and Kevin Han. Developing hazard recognition skill among the next-generation of construction professionals. *Construction management and economics*, 38(11): 1024–1039, 2020.
- Lynal Albert and Camren Routh. Designing impactful construction safety training interventions. *Safety*, 7(2):42, 2021.
- Yudistira Asnar and Nicola Zannone. Perceived risk assessment. In *Proceedings of the 4th ACM Workshop on Quality of Protection*, pages 59–64, 2008.
- Diane M Bunce, Elizabeth A Flens, and Kelly Y Neiles. How long can students pay attention in class? a study of student attention decline using clickers. *Journal of Chemical Education*, 87(12):1438–1443, 2010.
- Michael J Burke, Sue Ann Sarpy, Kristin Smith-Crowe, Suzanne Chan-Serafin, Rommel O Salvador, and Gazi Islam. Relative effectiveness of worker safety and health training methods. *American journal of public health*, 96(2):315–324, 2006.
- Michael J Burke, Rommel O Salvador, Kristin Smith-Crowe, Suzanne Chan-Serafin, Alexis Smith, and Shirley Sonesh. The dread factor: how hazards and safety training influence learning and performance. *Journal of applied psychology*, 96(1):46, 2011.
- Nishi Chaudhary, SM Uddin, Sathvik Sharath Chandra, Anto Ovid, and Alex Albert. Prompt to protection: A comparative study of multimodal llms in construction hazard recognition. *arXiv preprint arXiv:2506.07436*, 2025.
- Tom Cherrett, Gary Wills, Joe Price, Sarah Maynard, and Itiel E Dror. Making training more cognitively effective: Making videos interactive. *British Journal of Educational Technology*, 40(6):1124–1134, 2009.
- Jacob Cohen. *Statistical power analysis for the behavioral sciences*. routledge, 2013.
- Jonathan Cook, Tim Rocktäschel, Jakob Foerster, Dennis Aumiller, and Alex Wang. Ticking all the boxes: Generated checklists improve llm evaluation and generation. *arXiv preprint arXiv:2410.03608*, 2024.
- Elaine T Cullen. Tell me a story using stories to improve occupational safety training. *Professional Safety*, 53(07), 2008.

- Donald E Eggerth, Brenna M Keller, Thomas R Cunningham, and Michael A Flynn. Evaluation of toolbox safety training in construction: The impact of narratives. *American journal of industrial medicine*, 61(12):997–1004, 2018.
- Chinweike Eseonu, John Gambatese, and Chukwuma Nnaji. Reducing highway construction fatalities through improved adoption of safety technologies. *The Center for Construction Research Training: Silver Spring, MD, USA*, 2018.
- Konstantina Gkritza, Kumares C Sinha, Samuel Labi, and Fred L Mannering. Influence of highway construction projects on economic development: an empirical assessment. *The Annals of Regional Science*, 42(3):545–563, 2008.
- Harold Gomes, Vidisha Parasram, James Collins, and Christina Socias-Morales. Time series, seasonality and trend evaluation of 7 years (2015–2021) of osha severe injury data. *Journal of safety research*, 86:30–38, 2023.
- Google DeepMind. Gemini 2.5 flash. <https://ai.google.dev/models/gemini>, 2025a. Accessed: 2026-04-14.
- Google DeepMind. Gemini 3 pro. <https://deepmind.google/technologies/gemini/>, 2025b. Accessed: 2026-04-14.
- Google DeepMind. Introducing Nano Banana Pro. Google Blog, November 2025c. URL <https://blog.google/innovation-and-ai/products/nano-banana-pro/>. Accessed: 2026-02-26.
- Brian HW Guo, Yang Zou, Yihai Fang, Yang Miang Goh, and Patrick XW Zou. Computer vision technologies for safety science and management in construction: A critical review and future research directions. *Safety science*, 135:105130, 2021.
- Sungkook Hong, Byungjoo Choi, Youngjib Ham, JungHo Jeon, and Hyunsoo Kim. Massive-scale construction dataset synthesis through stable diffusion for machine learning training. *Advanced Engineering Informatics*, 62:102866, October 2024. ISSN 1474-0346. doi: 10.1016/j.aei.2024.102866.
- Jinwoo Jeon, JunHyeok Oh, Hayeong Lee, and Byung-Jun Lee. Iterative prompt refinement for safer text-to-image generation. In *Proceedings of the 2025 Conference on Empirical Methods in Natural Language Processing*, pages 18091–18107, 2025.
- Amita Kamath, Jack Hessel, and Kai-Wei Chang. What’s “up” with vision-language models? investigating their struggle with spatial reasoning. In *Proceedings of the 2023 Conference on Empirical Methods in Natural Language Processing*, pages 9161–9175, 2023.
- Mohammed Abdul Hafeez Khan, Yash Jain, Siddhartha Bhattacharyya, and Vibhav Vineet. Test-time prompt refinement for text-to-image models. In *Proceedings of the IEEE/CVF International Conference on Computer Vision*, pages 6506–6516, 2025.
- Hayoung Kim and June-Seong Yi. Image generation of hazardous situations in construction sites using text-to-image generative model for training deep neural networks. *Automation in Construction*, 166:105615, 2024.
- J Richard Landis and Gary G Koch. The measurement of observer agreement for categorical data. *biometrics*, pages 159–174, 1977.

- Jin Gang Lee, Jeongbin Hwang, Seokho Chi, and JoonOh Seo. Synthetic image dataset development for vision-based construction equipment detection. *Journal of Computing in Civil Engineering*, 36(5):04022020, 2022.
- Lujun Li, Lama Sleem, Niccolo' Gentile, Geoffrey Nichil, and Radu State. Exploring the impact of temperature on large language models: Hot or cold? *arXiv preprint arXiv:2506.07295*, 2025.
- Victor Weixin Liang, Yuhui Zhang, Yongchan Kwon, Serena Yeung, and James Y Zou. Mind the gap: Understanding the modality gap in multi-modal contrastive representation learning. *Advances in Neural Information Processing Systems*, 35:17612–17625, 2022.
- Richard J Light. Measures of response agreement for qualitative data: some generalizations and alternatives. *Psychological bulletin*, 76(5):365, 1971.
- Yujie Lu, Bo Liu, Wei Wei, Bo Xiao, Zhangding Liu, and Wensheng Li. Generating synthetic images for construction machinery data augmentation utilizing context-aware object placement. *Developments in the Built Environment*, 21:100610, 2025.
- Trevor Neece and Alessandro Fascetti. Comparative analysis of multimodal ai models for automated construction safety monitoring and reporting. *Journal of Computing in Civil Engineering*, 2026. doi: 10.1061/JCCEE5/CPENG-7383. In press.
- Trevor Neece, Mason Smetana, and Lev Khazanovich. Immersive technologies for occupational safety in horizontal transportation construction: A systematic review. *Applied Sciences*, 2026. Manuscript ID: applsci-4194328. Accepted for publication in the Special Issue “Emerging Technologies of Accident Analysis and Prevention in Safety Engineering”.
- Chukwuma Nnaji, John Gambatese, Hyun Woo Lee, and Fan Zhang. Improving construction work zone safety using technology: A systematic review of applicable technologies. *Journal of traffic and transportation engineering (English edition)*, 7(1):61–75, 2020.
- Mayu Otani, Riku Togashi, Yu Sawai, Ryosuke Ishigami, Yuta Nakashima, Esa Rahtu, Janne Heikkilä, and Shin'ichi Satoh. Toward verifiable and reproducible human evaluation for text-to-image generation. In *Proceedings of the IEEE/CVF Conference on Computer Vision and Pattern Recognition*, pages 14277–14286, 2023.
- Alec Radford, Jong Wook Kim, Chris Hallacy, Aditya Ramesh, Gabriel Goh, Sandhini Agarwal, Girish Sastry, Amanda Askell, Pamela Mishkin, Jack Clark, et al. Learning transferable visual models from natural language supervision. In *International conference on machine learning*, pages 8748–8763. PmLR, 2021.
- Jon Ricketts, David Barry, Weisi Guo, and Jonathan Pelham. A scoping literature review of natural language processing application to safety occurrence reports. *Safety*, 9(2):22, 2023.
- Edwin Sawacha, Shamil Naoum, and Daniel Fong. Factors affecting safety performance on construction sites. *International journal of project management*, 17(5):309–315, 1999. ISSN 0263-7863.
- Mason Smetana, Lucio Salles de Salles, Igor Sukharev, and Lev Khazanovich. Highway construction safety analysis using large language models. *Applied Sciences*, 14(4):1352, 2024.

- Mason Smetana, Lucio Salles de Salles, and Lev Khazanovich. Improving large language model assisted categorization and classification of highway construction accidents. *Engineering Applications of Artificial Intelligence*, 176:114798, 2026.
- Ornella Tanga, Opeoluwa Akinradewo, Clinton Aigbavboa, Ayodeji Oke, and Samuel Adekunle. Data management risks: a bane of construction project performance. *Sustainability*, 14(19):12793, 2022.
- Wei Tian, Hao Li, Hao Zhu, Yongwei Wang, Xianda Liu, Rongzheng Yang, Yujun Xie, Meng Zhang, Jun Zhu, and Xiangyu Wang. A review of smart camera sensor placement in construction. *Buildings*, 14(12):3930, 2024.
- Yujie Wei and Burcu Akinci. Synthetic image data generation for semantic understanding in everchanging scenes using bim and unreal engine. In *Computing in Civil Engineering 2021*, pages 934–941. 2021.
- Jinxian Weng and Qiang Meng. Analysis of driver casualty risk for different work zone types. *Accident Analysis & Prevention*, 43(5):1811–1817, 2011.
- James R Wilkins. Construction workers’ perceptions of health and safety training programmes. *Construction management and economics*, 29(10):1017–1026, 2011. ISSN 0144-6193.
- Work Zone Safety Information Clearinghouse. National & state traffic data: Work zone fatal crashes and fatalities, 2025. URL <https://workzonesafety.org/work-zone-data/work-zone-fatal-crashes-and-fatalities/>. Accessed: 2025-11-24.
- Bohan Xiao, Peiyong Wang, Qisheng He, and Ming Dong. Deterministic image-to-image translation via denoising brownian bridge models with dual approximators. In *Proceedings of the Computer Vision and Pattern Recognition Conference*, pages 28232–28241, 2025.
- Ruoxin Xiong and Pingbo Tang. Machine learning using synthetic images for detecting dust emissions on construction sites. *Smart and Sustainable Built Environment*, 10(3):487–503, 2021.
- Jialong Zuo, Haoyou Deng, Hanyu Zhou, Jiabin Zhu, Yicheng Zhang, Yiwei Zhang, Yongxin Yan, Kaixing Huang, Weisen Chen, Yongtai Deng, et al. Is nano banana pro a low-level vision all-rounder? a comprehensive evaluation on 14 tasks and 40 datasets. *arXiv preprint arXiv:2512.15110*, 2025.

A Prompt Templates

This section presents the complete set of prompt templates used in the image generation pipeline. Prompts are organized by generation stage. Placeholders enclosed in curly braces (e.g., `{json_data}`) denote runtime substitutions drawn from the OSHA SIR record D or from the output of a prior generation step.

A.1 LLM Text Generation Prompts

The following prompts are passed to the language model f_θ (Gemini 2.5 Flash) to generate the scene descriptions $\{R_{T1}, R_{T2}, R_{T3}, R_{T4}\}$ and T_{SP} .

State 1: Base Infrastructure (P_{T1})

You are a Prompt Engineer for an AI image generator. Describe the base infrastructure from this OSHA data: `{json_data}`.

Instruction: Write 3 sentences focusing on the roadway, terrain, or traffic control layout (barriers, cones, lane markings).

Pre-construction phase: There should be no construction equipment or workers described yet. Based on the Address and city, consider if this is an urban, highway, rural, or residential setting.

Constraint: Describe only the static environment. DO NOT include construction machines, vehicles, or workers.

Output Format: Plain text only. No preamble or markdown.

State 2: Construction Activity (P_{T2})

You are a Prompt Engineer for an AI image generator. Add equipment and workers to the existing environment: `{infrastructure_description}`.

Instruction: Write 3 sentences introducing the construction machines/vehicles and 1–2 workers performing the routine task from this OSHA data: `{json_data}`.

Focus: Mention equipment placement and worker positions relative to the infrastructure.

- Include PPE explicitly listed.
- Consider the health and safety hazard that will be introduced in the next step, but do not describe it yet. What type of construction activity would occur before this hazard takes place?
- Ensure that a worker, who will later interact with a hazard, is clearly depicted within the work zone.
- Ensure that any construction machines which will later be involved in the hazard are also present and correctly positioned.

Tone: Objective and routine. Do not describe any danger yet.

Output Format: Plain text only. No preamble.

State 3: Safety Warning Specification (P_{T3})

You are a Prompt Engineer for an AI image generator. Add a safety warning overlay to the existing scene: {activity_description}.

Instruction: Write 2–3 sentences that:

1. Identify which worker is in the danger zone and should be highlighted with a red outline or glow.
2. Generate a concise safety warning phrase (5–7 words max) based on the upcoming hazard from the OSHA data: {json_data}.

Safety Warning Examples:

- “Watch for pinch points”
- “Watch for tipping vehicles”
- “Maintain safe distance from equipment”
- “Watch for overhead hazards”
- “Stay clear of swing radius”
- “Watch for struck-by hazards”
- “Beware of fall hazards”

Output Format: Plain text only. No preamble.

Line 1: Description of which worker to highlight and their position.

Line 2: SAFETY_WARNING: [Your generated warning phrase]

State 4: Hazard Event (P_{T4})

You are a Prompt Engineer for an AI image generator. Add a hazard description to the existing scene: {activity_description}. Describe the peak of the hazard and physical interaction based on this data: {json_data}.

Instruction: Write 3 sentences capturing the moment the hazard becomes visible and the resulting physical interaction (e.g., impact or fall) between the worker and the threat.

Focus: Use the ‘event_keyword’ to define the specific threat and describe the mechanics of the event with forensic clarity.

Constraint: Do not dramatize. Stick to the physical description provided in the text.

Output Format: Plain text only. No preamble.

Single-Pass Scene Description (P_{SP})

You are a Prompt Engineer for an AI image generator. Generate a forensic, frozen-moment description of a safety incident: {json_data}.

Instruction: Structure your description into three distinct sections, leading with the specific labels below:

1. **THE INFRASTRUCTURE:** Describe the base roadway or work zone layout (e.g., pavement, lane markings, traffic control). No machines or workers.
2. **THE ACTIVITY:** Introduce the construction equipment and workers performing their routine task within that space.
3. **THE HAZARD:** Describe the peak of the event, focusing on the physical interaction between the worker and the hazard ({event_keyword}).

Constraints: 1–2 sentences per step. Start the response immediately with the Step 1 description. No dramatization or inventions.

Output Format: Output as a single cohesive paragraph. Plain text only. No preamble.

A.2 Image Generation Prompts

The following visual constraints prompts $\{V_{T1}, V_{T2}, V_{T3}, V_{T4}, V_{SP}\}$ are passed to the image generator f_G (Gemini 3 Pro) alongside the scene descriptions from Section A.1. The placeholder $\{\text{state_description}\}$ denotes the corresponding scene description R generated in the prior step.

State 1: Base Environment Image (V_{T1})

You are generating an image taken at eye-level, as if an inspector took the photo while standing a few feet away. The worker taking the photo should be standing within the traffic control or work zone.

Instruction: Generate a photorealistic educational visualization of a construction environment. This state acts as the base environment; do not add any construction equipment or workers. Only generate roadway, terrain, or traffic control layout (barriers, cones, lane markings) as specified in the description. The construction zone must have open space for work to occur.

Description: $\{\text{state_description}\}$

Crucial Constraints:

1. Style and Purpose: Use realistic photography with bright, even lighting suitable for an educational manual.
2. Minimize Clutter: The background should be relatively clean and minimalist. Only include equipment or structures explicitly mentioned in the description. Avoid random debris or complex textures that distract from the main subject area.
3. Text Rules: Do not include overlaid captions, watermarks, or UI elements. Text is only permitted if it appears naturally on environmental objects, such as safety signs, labels on equipment, or vehicle branding.
4. Do not have the GUI of Google Streetview overlaid on the image.

State 2: Construction Activity Image (V_{T2})

You are generating an image. Acting as a VFX editor for an educational series, modify the provided input image to integrate the next step of the safety sequence. This state introduces construction equipment and workers performing their routine task.

Modification Task (The Activity): {state_description}

CRITICAL POSITIONING REQUIREMENT:

The following hazard will occur in the next state: {hazard_description}

You **MUST** position the workers and equipment such that this hazard can realistically occur in the next image.

- Place the worker who will be involved in the hazard in a location and posture that makes the incident plausible.
- Position any equipment, vehicles, or objects involved in the hazard so they are oriented correctly for the event.
- Ensure spatial relationships (distances, angles, sight lines) support the described hazard mechanics.
- All added construction activity must be within the work zone.

Crucial Constraints for Consistency and Clarity:

1. Lock Camera: Maintain the exact camera angle, perspective, and lens focal length of the input image. Do not zoom, pan, or reframe the shot.
2. Focal Point: The new elements (workers and construction equipment) must be the sharpest and most distinct part of the image. The existing background should remain distinct but secondary to the action.
3. Clean Integration: Add the new elements seamlessly into the existing geometry without adding unnecessary environmental clutter around them.
4. Text Rules: No overlaid text, labels, or captions. Text must only exist on physical objects within the scene, such as hazard signs or worker PPE.
5. Although the critical positioning requirement describes the hazard, this image must not depict the hazard event itself.

State 3: Safety Warning Overlay Image (V_{T3})

You are generating an image. Acting as a VFX editor for an educational safety training series, modify the provided input image to add a safety warning overlay. This state highlights the worker in danger and displays a safety notice before the hazard occurs.

Worker Highlight Description: {state_description}

Crucial Constraints for Consistency and Clarity:

1. Lock Camera: Maintain the exact camera angle, perspective, and lens focal length of the input image. Do not zoom, pan, or reframe the shot.
2. Worker Highlight: Add a distinct red outline, glow, or semi-transparent red overlay around the worker identified as being in danger. The highlight should be clearly visible but not obscure the worker's details.
3. Safety Warning Banner: Display the safety warning text prominently in the upper or lower third of the image. Use a high-contrast format: white or yellow bold text on a red or dark background banner. The text should be large and readable. The safety warning text should start with "SAFETY WARNING".
4. Preserve Scene: Do not alter the existing workers, equipment, or environment. Only add the highlight effect and text overlay.
5. Educational Tone: The overall effect should resemble a training video freeze-frame or safety manual illustration with clear visual callouts.

State 4: Hazard Event Image (V_{T4})

You are generating an image. Acting as a VFX editor for an educational series, modify the provided input image to integrate the next step of the safety sequence. This state introduces the health and safety hazard and the worker's interaction with it.

Modification Task (The Hazard): {state_description}

Do not create any new workers; the hazard must involve an existing worker from the previous state.

Do not create new construction equipment; the hazard must involve existing equipment from the previous state.

Crucial Constraints for Consistency and Clarity:

1. Move Camera: Feel free to adjust the camera angle so that the health and safety hazard and worker interaction are clearly visible. Maintain a realistic eye-level perspective. Do not change background info.
2. Focal Point: The new elements (the hazard or the incident) must be the sharpest and most distinct part of the image. The existing background should remain distinct but secondary to the action.
3. Clean Integration: Add the new elements seamlessly into the existing geometry without adding unnecessary environmental clutter around them.
4. Text Rules: No overlaid text, labels, or captions. Text should only exist on physical objects within the scene, such as hazard signs or worker PPE.

Single-Pass Hazard Image (V_{SP})

You are generating an image taken at eye-level, as if an inspector took the photo while standing a few feet away. Generate a photorealistic educational visualization of a construction scenario.

Image Description: {state_description}

Crucial Constraints for Consistency and Clarity:

1. Lock Camera: Maintain the exact camera angle, perspective, and lens focal length of the input image. Do not zoom, pan, or reframe the shot.
2. Focal Point: The new elements (workers, the hazard, or the incident) must be the sharpest and most distinct part of the image. The existing background should remain distinct but secondary to the action.
3. Clean Integration: Add the new elements seamlessly into the existing geometry without adding unnecessary environmental clutter around them.
4. Text Rules: No overlaid text, labels, or captions. Text should only exist on physical objects within the scene, such as hazard signs or worker PPE.

B Evaluation Interface

Figure 6 provides a sample screenshot of the Google Form used as the evaluation platform for the expert-based review. Reviewers filled out this form twice for each OSHA narrative reviewed. The form instructs reviewers to simultaneously evaluate both images/sequences created for that OSHA narrative under that methodology.

The screenshot shows a Google Form with the following content:

Synthetic Image Comparison Grades - Temporal Sequences

Fill this out for comparison of the synthetic images Temporal Sequence grades

[Sign in to Google](#) to save your progress. [Learn more](#)

1. What is your name (Last, First)?

Your answer _____

2. What is the IDX of the IMIS for this row. Ignore leading zeros, IDX = "065" should be input at "65".

Your answer _____

3. **Processing Artifacts** - Is Sequence 1 free from generation artifacts (e.g., watermarks, unwanted text, or unintended photographer elements like hands, phones, or partial faces)? If no, describe the issue. This does not include the Pitt IRISE Logo.

Yes

Other: _____

4. **Processing Artifacts** - Is **Sequence 2** free from generation artifacts (e.g., watermarks, unwanted text, or unintended photographer elements like hands, phones, or partial faces)? If no, describe the issue. This does not include the Pitt IRISE Logo.

Yes

Other: _____

Figure 6: Sample image of the evaluation platform used by reviewers to evaluate the single-pass images and temporal sequences.

C Text and Image Example

This section walks through the text and image generation of one OSHA narrative. This narrative was chosen because it produced both highly rated and poorly rated images during the expert review. The fields most relevant to image generation for this narrative are reproduced below:

- `event_desc`: Employee Killed When Struck by Motor Vehicle
- `event_type`: Struck By
- `src_of_injury`: Windstorm/Lightning, etc. [administrative classification; hazard is vehicle intrusion]
- `event_keyword`: HEAD, HIGH WIND, TRAFFIC ACCIDENT, CONSTRUCTION, COLLISION, STRUCK BY, BRIDGE, MOTOR VEHICLE
- `degree_of_inj`: Fatal
- `abstract_text`: *“Employee #1, a highway bridge construction worker, was walking in a bar ditch that was approximately 20 to 25 feet from the shoulder of the road. A collision between two motor vehicles resulted in one of the vehicles departing the paved surface and striking and killing Employee #1 as he was walking by.”*

Mode I: Single-Pass Image Generation

The full record was passed to the text generator f_θ with the structured prompt P_{SP} , which instructs the model to define three narrative layers (infrastructure, activity, hazard) in 1–2 sentences each. The output R_{SP} is reproduced verbatim below:

Infrastructure layer.

“THE INFRASTRUCTURE: A multi-lane highway intersection, N. Loop 289 and Akron Access Road, features a paved surface bordered by a clear shoulder. Beyond the shoulder, a distinct bar ditch runs parallel to the roadway, approximately 20 to 25 feet from the paved edge.”

Activity layer.

“THE ACTIVITY: A highway bridge construction worker is performing a usual task, walking within the bar ditch. The worker maintains a position approximately 20 to 25 feet from the paved shoulder of the road.”

Hazard layer.

“THE HAZARD: On the adjacent paved surface, two motor vehicles collide, causing one vehicle to veer sharply from the roadway. This vehicle departs the paved surface, crosses the shoulder, and strikes the worker in the head within the bar ditch.”

The three layers are concatenated to form the complete description R_{SP} , which is then embedded in the visual constraints prompt V_{SP} . The single-pass image I_{SP} is produced twice using f_G and visualized in Figure 7. Because f_G is a stochastic generator, two statistically independent images from the same prompt were obtained. For Iteration 1 (see Figure 7 (A)), the image received unanimous reviews of “Major issues – not acceptable”. This was primarily because the two car accident is visible on the left side of the image, yet the car hitting the

worker is clearly coming from the right side of the image. However, Iteration 2 (see Figure 7 (B)) clearly depicts the vehicle collision, with one car veering into the median moments away from striking the worker.



Figure 7: Single-pass outputs of the example OSHA narrative. (A) Iteration 1 and (B) Iteration 2.

Mode II: Temporal Sequences

The temporal pipeline decomposed the OSHA narrative into four sequentially generated text descriptions $\{R_{T1}, R_{T2}, R_{T3}, R_{T4}\}$, each produced by f_{θ} conditioned on the prior output, which then drive a sequential image-to-image conditioning pipeline through f_G . As with the single-pass case, two statistically independent iterations of the full pipeline were executed from identical prompts.

State 1 — Base Environment (R_{T1})

The first description captures the static highway infrastructure with no workers or equipment present:

“The site features a wide, multi-lane paved highway, likely part of Loop 289, designed for significant traffic flow. A distinct shoulder borders the main roadway, giving way to a broad, unpaved bar ditch that stretches approximately 20 to 25 feet from the road’s edge. Permanent lane markings delineate the travel lanes, and the infrastructure suggests the presence of an existing or planned bridge structure over or under the main thoroughfare.”

State 2 — Construction Activity (R_{T2})

Conditioned on R_{T1} and D , the activity description $R_{T2} = f_{\theta}(P_{T2}(D_{323}, R_{T1}))$ introduces workers and equipment into the established scene:

“A large excavator is positioned near the edge of the bar ditch, its bucket resting on a pile of excavated earth, indicating recent or ongoing trenching work for drainage or utility lines. Further down the ditch, a compact track loader is preparing to grade a section of the unpaved surface, while a dump truck idles on a temporary access path off the shoulder, ready for material transport. A highway bridge construction worker, wearing a hard hat and a high-visibility vest, is routinely walking along the base of the broad bar ditch, approximately 20 feet from the paved shoulder, inspecting the ground conditions.”

State 3 — Safety Warning Annotation (R_{T3})

The warning specification $R_{T3} = f_{\theta}(P_{T3}(D_{323}, R_{T2}))$ branches from R_{T2} independently of R_{T4} , identifying the at-risk worker and supplying a concise warning phrase:

“The highway bridge construction worker, walking along the base of the broad bar ditch approximately 20 feet from the paved shoulder, should be highlighted with a red outline or glow.

SAFETY_WARNING: Watch for vehicles leaving roadway”

State 4 — Hazard Event (R_{T4})

The hazard description $R_{T4} = f_{\theta}(P_{T4}(D_{323}, R_{T2}))$ depicts the peak worker–hazard interaction:

“On the adjacent paved shoulder, a sudden collision occurs between two motor vehicles. One of the vehicles, now uncontrolled, departs the paved surface and travels into the broad bar ditch. The motor vehicle then strikes the highway bridge construction worker, who is walking along the ditch base, resulting in a fatal impact to the head.”

Each description is paired with its corresponding visual constraints prompt V_{Ti} and passed to f_G to produce images $\{I_{T1}, I_{T2}, I_{T3}, I_{T4}\}$, which are visualized in Figure 8. Sequence 1 (see Figure 8 (A)) received mixed reviews, primarily because the impacting vehicle approaches from an implausible angle inconsistent with the two-vehicle collision described in R_{T4} . One reviewer also flagged a processing artifact in I_{T1} : a partial photographer figure visible on the left side of the frame, which persisted through the remaining states due to the sequential image-to-image conditioning. Sequence 2 (see Figure 8 (B)) received unanimous “No Issues — Fully Acceptable” ratings, with both reviewers awarding 5/5 for fidelity and alignment, citing a clear and accurate depiction of the collision event.

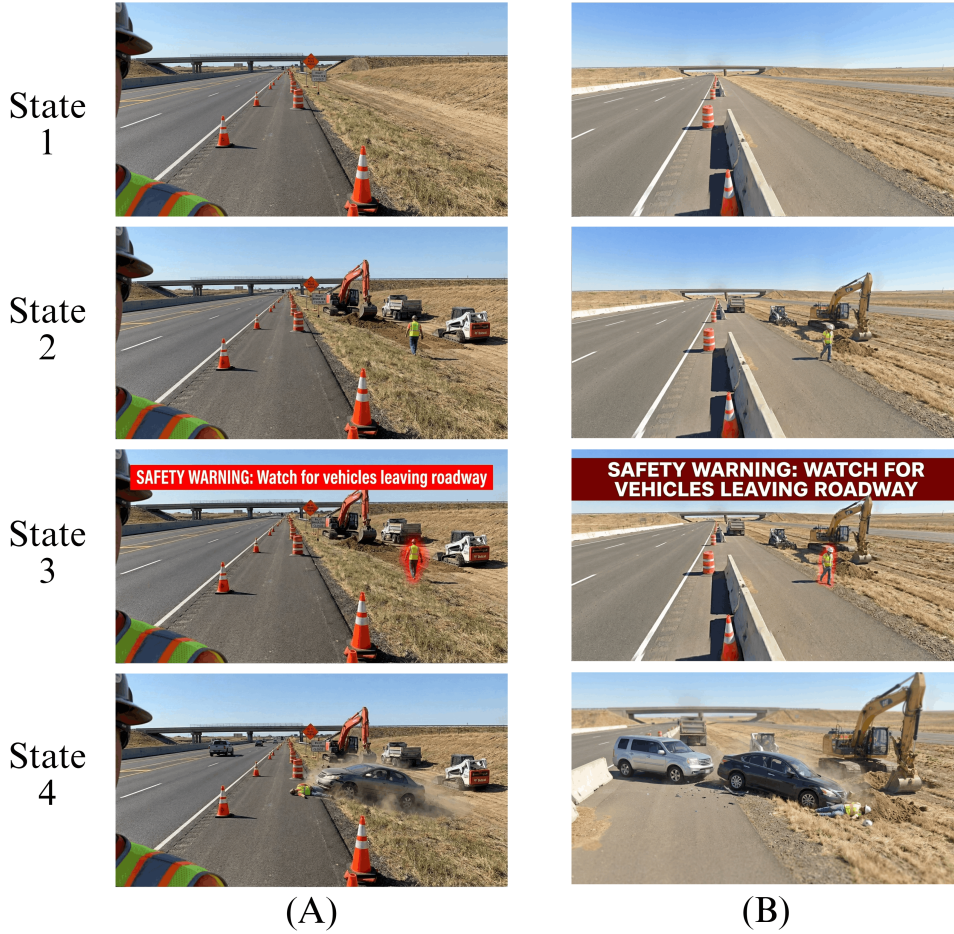


Figure 8: Temporal sequence outputs of the example OSHA narrative. (A) Iteration 1 and (B) Iteration 2. Each row shows the four frames: State 1, State 2, State 3, and State 4.

D Additional Results

Table 3: Distributional separation between matched and mismatched cosine similarities in CLIP space. Cohen’s d uses the pooled standard deviation. **MW** p is the one-sided Mann-Whitney U test against the null that matched similarities are no greater than mismatched.

Group	Mismatched		Matched		Sep.	Cohen’s d	MW p
	n	$\mu \pm \sigma$	n	$\mu \pm \sigma$			
Overall	22,200	0.178 ± 0.044	300	0.243 ± 0.043	1.48σ	1.545	1.22×10^{-106}
Single-pass	11,100	0.176 ± 0.043	150	0.249 ± 0.040	1.69σ	1.755	2.90×10^{-63}
Temporal	11,100	0.180 ± 0.045	150	0.237 ± 0.044	1.27σ	1.366	7.07×10^{-47}

Table 4: Supporting expert-evaluation data. (A) Inter-rater agreement (Light’s κ) by checklist dimension, with Landis-Koch agreement-strength labels. (B) Full educational utility breakdown: percent of evaluations in each of the three rating tiers (Fully Acceptable / Minor Issues / Major Issues), pooled across both stochastic iterations. (C) Stochastic recovery from paired comparative evaluations. Mean absolute reviewer disagreement on Likert scales: Single-Pass fidelity 0.84, alignment 0.89; Temporal fidelity 0.99, alignment 1.00.

(A) Inter-rater agreement (Light’s κ)

Dimension	κ		Agreement	
	Single-Pass	Temporal	Single-Pass	Temporal
Processing Artifacts	0.428	0.729	Moderate	Substantial
Hazard Accuracy	0.286	0.348	Fair	Fair
Scene Realism	0.167	0.135	Slight	Slight
Visual Coherence	0.148	0.232	Slight	Fair
Temporal Consistency	—	0.430	—	Moderate
Hazard Alert Accuracy	—	0.346	—	Fair

(B) Educational utility: full distribution and checklist failure rates

Dimension	Single-Pass (%)			Temporal (%)		
	Fully	Minor	Major	Fully	Minor	Major
Processing Artifacts	2.5	6.1	11.1	5.4	20.2	20.5
Hazard Accuracy	1.3	58.8	93.7	4.3	28.1	75.8
Scene Realism	7.0	32.5	36.5	23.9	56.1	51.5
Visual Coherence	2.5	23.7	17.5	6.5	15.8	28.8
Temporal Consistency	—	—	—	9.8	41.2	61.4
Hazard Alert Accuracy	—	—	—	4.3	9.6	26.5
<i>Rating share</i>	47.0	34.1	18.9	27.2	33.7	39.1

(C) Stochastic recovery from paired evaluations

Outcome	Single-Pass (%)	Temporal (%)
Both acceptable	70.1	44.0
Mixed	22.2	33.3
Both rejected	7.8	22.6
Recovery rate	74.0	59.6

E Image generation cost

The cost to create this dataset, as of February 2026, was \$0.30 per million tokens up and \$2.50 per million tokens down for Gemini 2.5 flash, while Gemini 3 Pro costs \$2.00 per million tokens up and \$12.00 per million tokens down, in addition to a \$0.134 baseline fee for high-resolution image generation.